

REPORT

COMMUNITY ECOLOGY

Emergent phases of ecological diversity and dynamics mapped in microcosms

Jiliang Hu^{1,2}, Daniel R. Amor^{1†}, Matthieu Barbier^{3,4}, Guy Bunin⁵, Jeff Gore^{1*}

From tropical forests to gut microbiomes, ecological communities host notably high numbers of coexisting species. Beyond high biodiversity, communities exhibit a range of complex dynamics that are difficult to explain under a unified framework. Using bacterial microcosms, we performed a direct test of theory predicting that simple community-level features dictate emergent behaviors of communities. As either the number of species or the strength of interactions increases, we show that microbial ecosystems transition between three distinct dynamical phases, from a stable equilibrium in which all species coexist to partial coexistence to emergence of persistent fluctuations in species abundances, in the order predicted by theory. Under fixed conditions, high biodiversity and fluctuations reinforce each other. Our results demonstrate predictable emergent patterns of diversity and dynamics in ecological communities.

In nature, species reside and interact with myriad other species in complex communities (1). Central challenges in ecology include understanding how many species are able to coexist, why biodiversity is higher in some places than others, why communities show varying dynamical behaviors (2, 3), and how these factors shape ecosystem functioning (4). A long-standing debate concerns whether the diversity of a community enhances or weakens its stability (5). By studying natural communities, ecologists have identified potential environmental drivers that could affect both biodiversity and community dynamics (6). Laboratory experiments facilitate disentangling such environmental drivers from inherent community properties, such as species interactions, that may also shape biodiversity and dynamics. Experimental communities with few species have been shown to display predictable dynamics, such as stable equilibria and periodic oscillations (7–11), and have allowed an understanding of the role of interactions ranging from predation (9–11) to competition (7, 8) to cross-feeding (12). In more biodiverse laboratory microcosms derived from natural habitats, however, community composition is only reproducible and predictable at family or higher levels of taxonomy (3, 13–15). Given the relative inaccessibility of detailed information on the ecological roles of every spe-

cies (capturing every interaction strength, growth rate, and carrying capacity, among others), the question arises: Is it possible to predict the biodiversity and dynamics of these complex communities with simple community-level parameters?

Starting with the pioneering work by Robert May (16), ecologists have sought to predict community behaviors using community-level parameters such as the number of species and the distribution of interaction strengths between species. The interaction strengths quantify how strongly a species influences the growth and survival of other organisms in the community and therefore determines the overall composition and stability of communities (14). May and others have suggested that a large number of species and strong interactions lead to instability of community dynamics (16–20), yet we still do not understand how communities behave beyond the transition to instability. Recent theory suggests that a fraction of species tend to go extinct before the community loses stability (21–23) and that unstable communities can exhibit fluctuations, which could in turn reinforce biodiversity (24–30). This body of theory has been difficult to validate because the associated parameters are hard to estimate and manipulate (31). Experimental microcosms have now reached the necessary controllability (8, 14, 15) to test theoretical predictions based on community-level parameters of ecological communities. We aim to uncover the relationship between stability and diversity through experimentally controlling two factors that are usually unobservable in natural settings: the strength of interspecies interactions and the number of species introduced in the experiment (referred to as the species pool size).

We began by summarizing the predictions on community dynamics and biodiversity from the well-known generalized Lotka-Volterra model, modified to include dispersal from a species pool:

$$\frac{dN_i}{dt} = N_i \left(1 - \sum_{j=1}^S a_{ij} N_j \right) + D \quad (1)$$

where N_i is the abundance of species i (normalized to its carrying capacity), a_{ij} is the interaction strength that captures how strongly species j inhibits species i (with self-regulation $a_{ii} = 1$), and D is the dispersal rate. We simulated the dynamics of communities with different species pool sizes S and interaction matrices. We sampled the interaction strength from a uniform distribution $U[0, 2\langle\alpha_{ij}\rangle]$, where $\langle\alpha_{ij}\rangle$ is the mean interaction strength between species (which also determines the variance of interactions; the values of $\langle\alpha_{ij}\rangle$ and $\text{std}(\alpha_{ij})$ increase proportionally in this study, where $\text{std}(\alpha_{ij})$ is the standard deviation of interactions; see (32)). Modeling species interactions as a random interaction network captures species heterogeneity without assuming any particular community structure (16, 17, 23).

Our simulations revealed a strong dependence of biodiversity (number of coexisting species) and dynamics on both the species pool size S (Fig. 1A) and interaction strength $\langle\alpha_{ij}\rangle$ (Fig. 1B). As either of these parameters increase, communities experience a transition from stable full coexistence (phase I: all species survive and reach stable abundances) to stable partial coexistence (phase II: some species go extinct, and the surviving ones reach stability) to persistent fluctuations in species abundances and biomass (phase III) [figs. S1 to S3 and (32)]. The transition to unstable dynamics (phase II to phase III) corresponds with the loss of linear stability of the equilibrium, consistent with May's theory (fig. S4). These results agree with recent theory that derived analytically the existence of a phase transition from a distinct stable state (phases I and II) to persistent fluctuations (phase III) (21, 22).

To address the ecological implications of these dynamical phases, we analyzed both the fraction of species that survive at equilibrium (Fig. 1, C and E, and fig. S5) and the fraction of communities that exhibit persistent fluctuations (Fig. 1, D and F). We found that the sequence of dynamical phases is generic across the parameter space: Communities generally experience species extinctions before they lose stability as either of the control parameters increase. This sequence is both predicted by analytical expressions for the phase boundaries (Fig. 1, C to F) and robust to different choices of interaction strength distributions

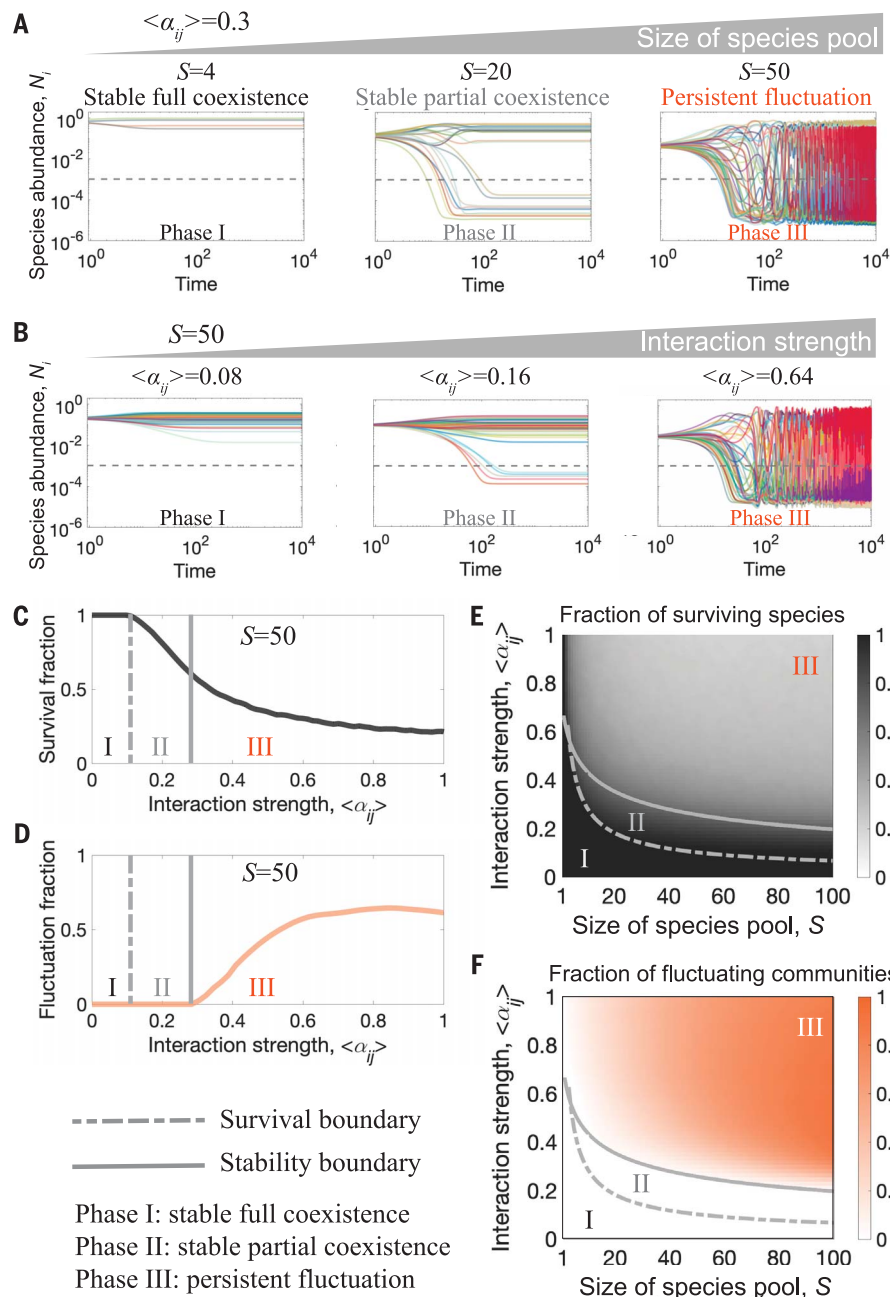
¹Physics of Living Systems, Department of Physics, Massachusetts Institute of Technology, Cambridge, MA 02139, USA. ²Department of Mechanical Engineering, Massachusetts Institute of Technology, Cambridge, MA 02139, USA. ³CIRAD, UMR PHIM, 34090 Montpellier, France. ⁴PHIM Plant Health Institute, University of Montpellier, CIRAD, INRAE, Institut Agro, IRD, 34090 Montpellier, France. ⁵Department of Physics, Technion—Israel Institute of Technology, Haifa 3200003, Israel.

*Corresponding author. Email: gore@mit.edu

[†]Present address: Institute of Biology, University of Graz, A-8010 Graz, Austria.

Fig. 1. Theory predicts that species pool size and interspecies interaction strength shape phases of community diversity and dynamics.

(A) Representative time series of species abundance for the qualitatively different dynamics of communities with different species pool size S , under interaction strength $\langle\alpha_{ij}\rangle = 0.3$. Communities transition from stable full coexistence ($S = 4$) to stable partial coexistence ($S = 20$) to persistent fluctuations ($S = 80$). (B) Increasing interaction strength while fixing the species pool size reveals analogous transitions. The values of $\langle\alpha_{ij}\rangle$ and $\text{std}(\alpha_{ij})$ increase proportionally in this study. (C and D) Mean fractions of species that survive in the community (C) and communities that exhibit persistent fluctuations (D). As interaction strength increases, communities lose species (dashed vertical line, transition from phase I to phase II) before losing stability (solid vertical line, transition from phase II to phase III). (E and F) Mapping the survival fraction (E) and community fluctuation fraction (F) onto the phase space reveals that this sequence (phase I to phase II to phase III) of phase transitions is maintained as either of the control parameters increases. The gray dashed (solid) line shows the analytical solution for the survival (stability) boundary. The color maps depict the mean value over 1000 simulations (32).



and modeling assumptions (figs. S6 and S7) (27). In particular, natural ecological communities display diverse interaction types, which affects the degree of symmetry in the interaction matrix (α_{ij}) (e.g., competition and mutualism may be symmetrical, whereas predation is antisymmetrical). We found that varying these properties of the interaction matrix does not qualitatively affect the dynamical phases (figs. S8 and S9). Other model choices—for example, considering pH-mediated interactions or the serial dilution of communities into fresh media (figs. S9 to S12) (14)—further showed the robustness

and generic nature of the dynamical phases. Therefore, it may be possible to predict the diversity and dynamics of ecological communities from community-level features of the interaction network.

To experimentally test the predicted phase transitions, we built synthetic communities using a library of 48 bacterial isolates from terrestrial environments [figs. S13 and S14 and (32)]. After inoculation, we exposed communities to cycles of growth, dispersal from the pool, and dilution while monitoring community composition and biomass at the end of each daily cycle [Fig. 2A and (32)]. Leverag-

ing previous work (14, 33), we tested media conditions to tune the strength of bacterial interactions. We found that the probability of coexistence in pairwise coculture decreased with the concentration of supplemented glucose and urea. In this medium, an increase in the concentration of these nutrients therefore increases the strength of competitive interactions (Fig. 2B and tables S1 to S3). As discussed in our previous work (14, 33), high nutrient concentrations lead to extensive modification of the media (e.g., pH) and hence stronger interactions. This experimental platform allows us to control the key parameters

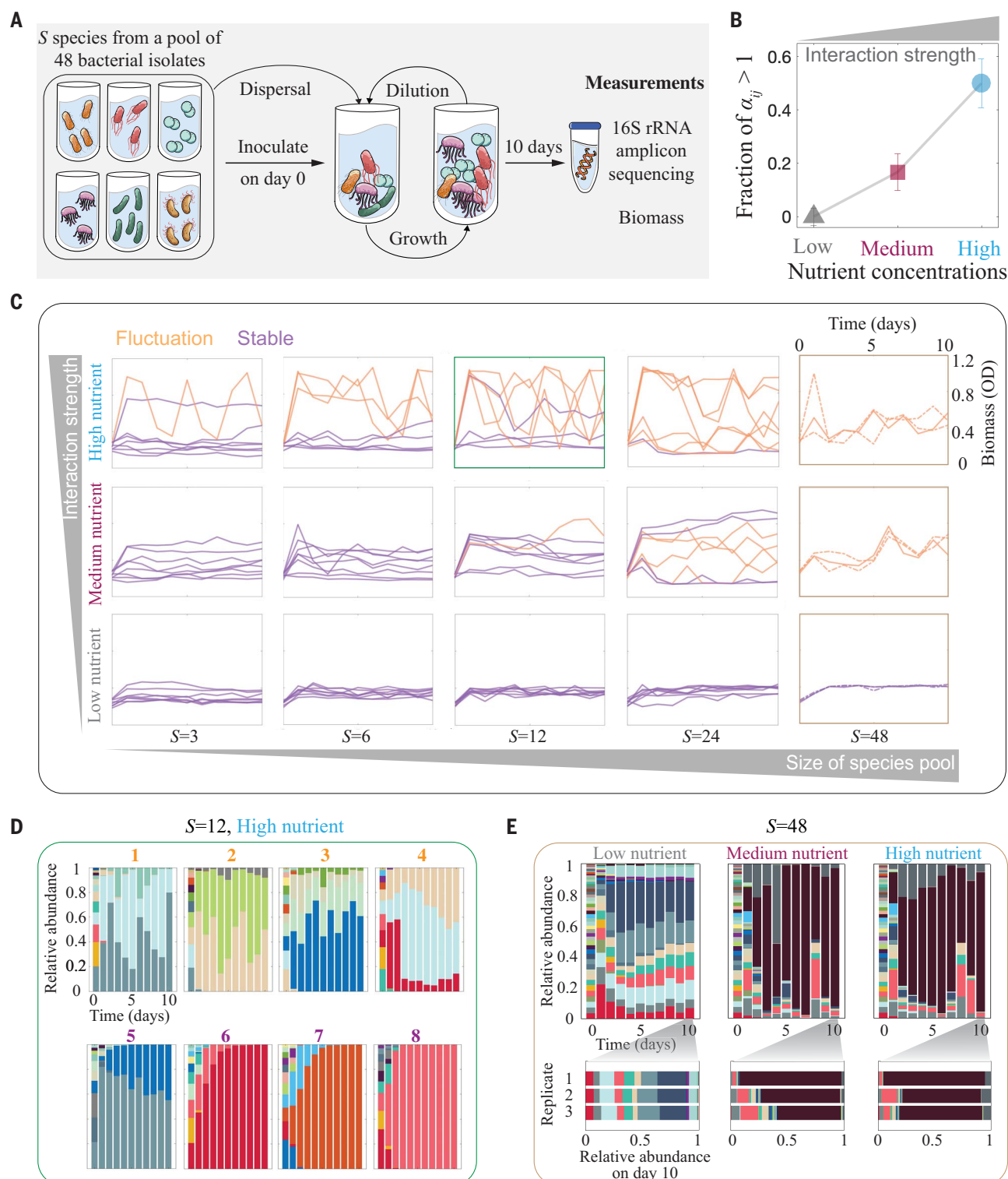


Fig. 2. Increasing species pool size or interaction strength leads to loss of stability in microbial communities. (A) We used a library of 48 bacteria to generate species pools of different sizes and compositions. Cocultures underwent serial dilutions with additional dispersal from the pool. Community composition and total biomass were monitored through 16S sequencing and optical density (OD). (B) In two-species cocultures, interaction strengths leading to the loss of coexistence ($\alpha_{ij} > 1$) increase in frequency with nutrient concentration. Error bars represent SEM; $n = 30$. (C) Fluctuations in community biomass increase with either species pool size or interaction strength. Solid lines represent eight

different species pool compositions (dashed lines represent replicates of the 48-species community). Purple (orange) lines highlight stable (fluctuating) dynamics. (D) Under high nutrient concentration, half of the 12-species communities exhibit persistent fluctuations (top panels) in species abundances and the rest reached stability (bottom panels). (E) Time series (top panels) for the species abundances in 48-species communities. Stability was reached only under low nutrient concentration, and variability in end-point relative abundances increased with nutrient concentration (bottom panels) (fig. S15). Relative abundance plots show the amplicon sequence variant data of individual replicates.

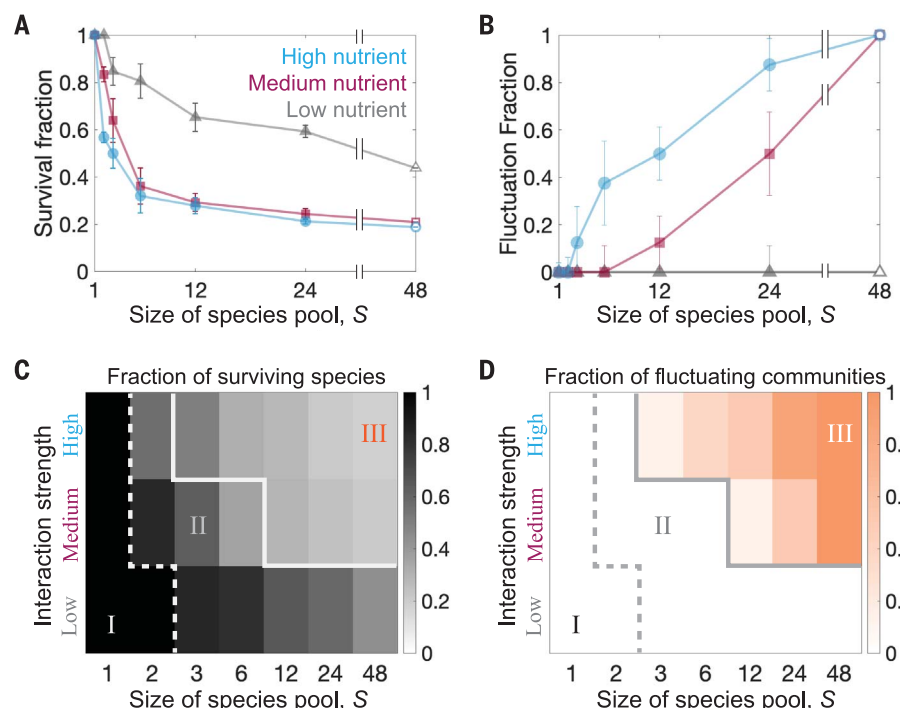


Fig. 3. Species pool size and interaction strength determine the diversity and dynamics of experimental communities. (A) Fraction of surviving species decreases with either species pool size or interaction strength (nutrient concentration). The survival fraction decreases more slowly at high S and strong interaction strength. (B) Fraction of fluctuating communities increases with either species pool size or interaction strength. (C) Phase diagram for the fraction of species surviving in experimental communities. As communities cross the boundary of phase I (dashed white line), they experience species extinctions, with a fast decay in survival fraction through phase II and a relative maintenance of survival fraction through phase III. The solid white line indicates the stability boundary. (D) Phase diagram for the fraction of fluctuating communities in experiments. Communities start exhibiting persistent fluctuations after crossing the boundary into phase III (solid gray line). The dashed gray line indicates the survival boundary. In (A) and (B), error bars represent SEM; $n = 8$.

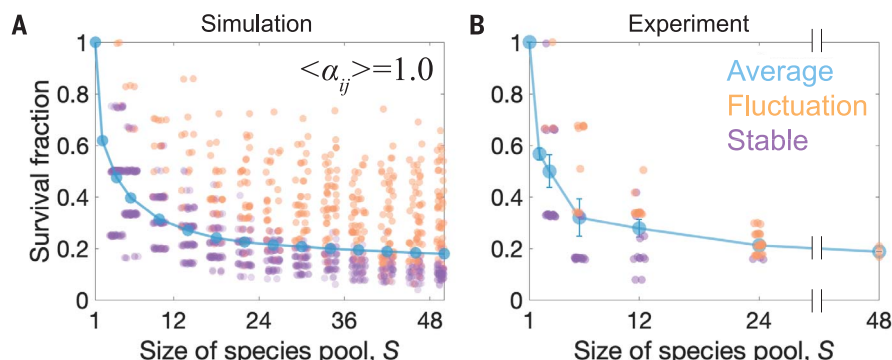


Fig. 4. Fluctuating communities are more diverse than stable communities under the same conditions. (A) As the average survival fraction (blue line) decreases with increasing species pool size S in simulations, more communities exhibit fluctuations in species abundances (orange data points). Whereas stable communities (purple data points) exhibit a steady decrease in species survival fraction with S , the loss of species is slower in fluctuating communities. Each data point represents an individual community. (B) In experiments under high nutrient concentration (also under lower nutrient concentration; fig. S28), fluctuating communities exhibit a higher survival fraction than stable communities. The survival fractions of 88% ($\pm 5\%$) of the fluctuating communities are above or equal to the mean, as compared with 14% ($\pm 6\%$) in the case of stable communities [$p < 0.01$; (32)]. Error bars represent SEM; $n = 8$.

established by theory: species pool size and interaction strength.

We experimentally mapped the phase space of community dynamics by exposing 63 species pools to three levels of interaction strength. Specifically, we tested 30 species pairs ($S = 2$); eight different communities for each size $S = 3, 6, 12$, and 24 ; and one community of $S = 48$ (the full species library). The resulting biomass time series were relatively stable under low interaction strength and small species pool size, whereas increasing these two variables progressively led to a higher fraction of communities exhibiting biomass fluctuations (Fig. 2C). Analyzing species abundances through 16S sequencing (Fig. 2, D and E), we found that biomass fluctuations were highly correlated with species abundance fluctuations (figs. S15 and S16). For example, for communities with 12 species in the pool and high nutrient concentration, four communities reached stable equilibria and the remaining four exhibited fluctuations in both biomass and species abundances until the end of the experiment (Fig. 2, C and D). Replicates with identical species pool composition exhibited highly reproducible dynamics (figs. S17 to S25), and the classification of stable and fluctuating communities was robust to different methods that analyzed biomass, species composition, and variations between replicates [figs. S15 and S16 and (32)]. We also experimentally observed this transition toward unstable dynamics under different carbon sources and dilution frequencies (fig. S27). Therefore, synthetic microbial communities lose stability as either species pool size (for $S > 2$) or interaction strength increases.

To understand the relationship between species extinctions and loss of community stability, we analyzed species survival across these experiments. As expected, the fraction of surviving species decreased with an increase in either species pool size or interaction strength, as determined by nutrient concentration (Fig. 3A). For example, at medium interaction strength, 83% ($\pm 3\%$) of species were able to survive in the 30 pairwise ($S = 2$) cocultures, whereas this frequency decreased to 36% ($\pm 7\%$) among the eight different combinations of six-species communities ($S = 6$; Fig. 3A). Despite the pronounced loss of species, none of these communities displayed persistent fluctuations (Fig. 3B). Such fluctuations arose with further increase of the species pool size, with half of the 24-species combinations displaying fluctuations (Fig. 3B). Notably, the species survival fraction displayed only a modest decrease entering the fluctuation regime, with 24% ($\pm 2\%$) of species surviving in the 24-species communities as compared with 36% ($\pm 7\%$) in the six-species communities (Fig. 3, A and B). Mapping these experimental results over the phase space (Fig. 3, C and D) confirmed the theoretically predicted (Fig. 1, E and F) sequence of transitions:

Communities experience species extinctions before exhibiting persistent fluctuations, as either species pool size or interaction strength increases.

Next, through analyzing species survival fraction across different species pool compositions, we addressed how fluctuations and diversity may influence each other. In simulations, the fraction of surviving species revealed a generic trend: For the same species pool size and interaction strength, fluctuating communities were more diverse than stable communities (Fig. 4A). This trend was also observed in experiments: Most fluctuating communities reached higher survival fractions than stable communities reached under the same conditions (Fig. 4B and fig. S28). For example, within the 12-species communities, fluctuating communities had on average 5 ± 1 species surviving, as compared with only 2 ± 1 species surviving in stable communities. Among the fluctuating communities, 88% ($\pm 5\%$) exhibited survival fractions above or equal to the mean, as compared with only 14% ($\pm 6\%$) among the stable communities [$p < 0.01$; (32)]. Both experiments and simulations suggest that fluctuations are an emergent, diversity-dependent phenomenon, because the addition of species pools from stable communities often yielded larger, fluctuating communities (fig. S29). We also found numerically that fluctuations and high diversity disappeared together as we stopped dispersal or pinned the abundance of the most abundant species (fig. S1). Our results show that diversity and persistent fluctuations enhance each other, as theoretically demonstrated in previous work (25, 26).

Our findings are consistent with two major ideas in theoretical ecology: May's suggestion that complexity leads to instability (16) and Chesson's argument that temporal fluctuations can help maintain diversity (34). The question of whether complex dynamics are inherent to the ecological community—arising from species interactions—or driven by environmental factors has received considerable attention yet has seldom undergone a direct experimental test in many-species communities. Under laboratory conditions that minimize environmental stochasticity, and in agreement with recent theory (21, 23, 35), we found that community-level parameters representing

species diversity and interactions are sufficient to predict the dynamical behaviors of complex ecological communities. These predictions are theoretically robust to varying biological assumptions [e.g., intraspecific diversity and interspecies interaction mechanisms, including resource-explicit models (36)]. Therefore, the emergent phases of biodiversity and dynamics that we observed in this study may occur in a wide range of ecological communities. Future work should study whether these phases generalize across spatiotemporal scales, environmental conditions, and organism types to understand their prevalence and importance in shaping major ecological patterns (37, 38).

REFERENCES AND NOTES

1. R. M. May, *Science* **241**, 1441–1449 (1988).
2. J. J. Faith *et al.*, *Science* **341**, 1237439 (2013).
3. E. Benincà, B. Ballantine, S. P. Ellner, J. Huisman, *Proc. Natl. Acad. Sci. U.S.A.* **112**, 6389–6394 (2015).
4. G. W. Luck, G. C. Daily, P. R. Ehrlich, *Trends Ecol. Evol.* **18**, 331–336 (2003).
5. K. S. McCann, *Nature* **405**, 228–233 (2000).
6. A. R. Ives, S. R. Carpenter, *Science* **317**, 58–62 (2007).
7. J. Friedman, L. M. Higgins, J. Gore, *Nat. Ecol. Evol.* **1**, 109 (2017).
8. O. S. Venturelli *et al.*, *Mol. Syst. Biol.* **14**, e8157 (2018).
9. F. K. Balagaddé *et al.*, *Mol. Syst. Biol.* **4**, 187 (2008).
10. B. Blasius, L. Rudolf, G. Weithoff, U. Gaedke, G. F. Fussmann, *Nature* **577**, 226–230 (2020).
11. G. F. Fussmann, S. P. Ellner, K. W. Shertzer, N. G. Hairston Jr., *Science* **290**, 1358–1360 (2000).
12. W. Shou, S. Ram, J. M. G. Vilar, *Proc. Natl. Acad. Sci. U.S.A.* **104**, 1877–1882 (2007).
13. E. Benincà *et al.*, *Nature* **451**, 822–825 (2008).
14. C. Ratzke, J. Barrere, J. Gore, *Nat. Ecol. Evol.* **4**, 376–383 (2020).
15. J. E. Goldford *et al.*, *Science* **361**, 469–474 (2018).
16. R. M. May, *Nature* **238**, 413–414 (1972).
17. S. Allesina, S. Tang, *Nature* **483**, 205–208 (2012).
18. U. Bastolla *et al.*, *Nature* **458**, 1018–1020 (2009).
19. E. Thébaud, C. Fontaine, *Science* **329**, 853–856 (2010).
20. A. Mougi, M. Kondoh, *Science* **337**, 349–351 (2012).
21. G. Bunin, *Phys. Rev. E* **95**, 042414 (2017).
22. M. Oppen, S. Diederich, *Phys. Rev. Lett.* **69**, 1616–1619 (1992).
23. D. A. Kessler, N. M. Shnerb, *Phys. Rev. E* **91**, 042705 (2015).
24. J. Huisman, F. J. Weissing, *Nature* **402**, 407–410 (1999).
25. M. T. Pearce, A. Agarwala, D. S. Fisher, *Proc. Natl. Acad. Sci. U.S.A.* **117**, 14572–14583 (2020).
26. F. Roy, M. Barbier, G. Biroli, G. Bunin, *PLOS Comput. Biol.* **16**, e1007827 (2020).
27. J. C. Allen, W. M. Schaffer, D. Rosko, *Nature* **364**, 229–232 (1993).
28. R. V. Solé, D. Alonso, A. McKane, *Philos. Trans. R. Soc. London Ser. B* **357**, 667–671 (2002).

29. J. D. Touboul, A. C. Staver, S. A. Levin, *Proc. Natl. Acad. Sci. U.S.A.* **115**, E1336–E1345 (2018).
30. A. Hastings, C. L. Hom, S. Ellner, P. Turchin, H. C. J. Godfray, *Annu. Rev. Ecol. Syst.* **24**, 1–33 (1993).
31. D. S. Maynard, Z. R. Miller, S. Allesina, *Nat. Ecol. Evol.* **4**, 91–100 (2020).
32. Materials and methods are available as supplementary materials.
33. C. Ratzke, J. Gore, *PLOS Biol.* **16**, e2004248 (2018).
34. P. Chesson, *Theor. Popul. Biol.* **45**, 227–276 (1994).
35. M. Barbier, J. F. Arnoldi, G. Bunin, M. Loreau, *Proc. Natl. Acad. Sci. U.S.A.* **115**, 2156–2161 (2018).
36. I. Dalmedigos, G. Bunin, *PLOS Comput. Biol.* **16**, e1008189 (2020).
37. J. D. O'Sullivan, J. C. D. Terry, A. G. Rossberg, *Nat. Commun.* **12**, 3627 (2021).
38. Y. Yonatan, G. Amit, J. Friedman, A. Bashan, *Nat. Ecol. Evol.* **6**, 693–700 (2022).
39. J. Hu, D. R. Amor, M. Barbier, G. Bunin, J. Gore, Code from the manuscript "Emergent phases of ecological diversity and dynamics mapped in microcosms." Zenodo (2022); <https://doi.org/10.5281/zenodo.7017202>.

ACKNOWLEDGMENTS

We thank all the Gore Lab members for inspiring discussions. We thank M. Dal Bello at MIT for drawing the cartoons of bacterial cells. We also thank C. Ratzke, currently at the University of Tübingen, for the isolation of bacterial species, as well as the Eric Alm laboratory at MIT for sharing laboratory equipment. We thank the groups led by D. Fisher at Stanford, O. Hallatschek at UC Berkeley, and N. Shnerb and D. Kessler at Bar-Ilan University for valuable discussions. **Funding:** J.G. acknowledges support from the Alfred P. Sloan Foundation and Schmidt Polymath Award. G.B. acknowledges support from the Israel Science Foundation (ISF). D.R.A. acknowledges support from the Field of Excellence "Complexity in Life, Basic Research and Innovation" at the University of Graz. **Author contributions:** J.H. and J.G. conceived the study. J.H. and D.R.A. performed the experiments. J.H., M.B., and G.B. performed the theoretical modeling. All authors analyzed the data and wrote the manuscript. **Competing interests:** The authors declare that they have no competing interests. **Data and materials availability:** Isolates and communities are available upon request. All data are available in the supplementary materials. All codes used for simulation and analysis in this publication are available on GitHub (<https://github.com/Jiliang-Hu/Emergent-phases>) and Zenodo (39). **License information:** Copyright © 2022 the authors, some rights reserved; exclusive licensee American Association for the Advancement of Science. No claim to original US government works. <https://www.science.org/about/science-licenses-journal-article-reuse>

SUPPLEMENTARY MATERIALS

science.org/doi/10.1126/science.abm7841
Materials and Methods
Figs. S1 to S31
Tables S1 to S3
References (40–47)
MDAR Reproducibility Checklist
Data S1

[View/request a protocol for this paper from Bio-protocol.](#)

Submitted 28 October 2021; accepted 24 August 2022
10.1126/science.abm7841